Experimental Mechanics (2022) 62:677–683
https://doi.org/10.1007/s11340-021-00810-w

RESEARCH PAPER

An Equal-Biaxial Test Device for Large Deformation in Cruciform Specimens

M. Ru[1,2] · X.Q. Lei[1] · X.M. Liu[1,3] · Y.J. Wei[1,2,3]

Received: 4 July 2021 / Accepted: 24 November 2021 / Published online: 9 January 2022

Abstract

Background Biaxial tests are important for complex mechanical behaviours of materials such as rubbers, soft materials, polymers and bio-materials, and commercial biaxial testing machines are usually expensive.

Objective For convenience and cost control, an equal-biaxial device for soft materials, with a load capacity up to 100 N and a maximum displacement of 50 mm, is designed and manufactured.

Methods A novel rope and pulley load system is applied in the designed biaxial device, and the device ensures automatically equal stress in two directions and minimizes possible installation deviation. The biaxial strain is measured from the central zone of the cruciform samples by a set of non-contact laser extensometer.

Results The device is calibrated through an array of tests for three different types of soft materials, silicon rubber, polyimide (PI) and polyethylene terephthalate (PET). The repeatability of equal-biaxial strain–stress curves of the three materials is excellent. Possible error sources of the device are examined and their respective contributions are quantified.

Conclusions Such a device offers a convenient way to carry out biaxial tests for many materials such as rubbers, polymers, and biomaterials.

Keywords Biaxial tension · Soft matter · Cruciform specimen · Digital image correlation · Rope and pulley

Introduction

The mechanical properties of soft materials are of paramount importance for their usage in advanced devices, which are commonly acquired by uniaxial tensile test, biaxial tensile test, compression test, and so on. Uniaxial test can only obtain parameters associated with one stress component. For rubber like polymers where deformation is highly nonlinear, and very likely hydrostatic stress plays an important role, uniaxial tension is not sufficient. More complex tests are needed, such as shear test, pressured uniaxial test or biaxial test. Biaxial tests extend the stress analysis domain into planes of the principal stress space, and are widely developed and adapted in the analysis of many complex deformation mechanisms of material. Makinde in 1992 [1] reviewed the development of apparatus for biaxial tests using cruciform specimens. Kuwabara in 2007 [2], Hannon in 2008 [3], Merklein in 2013 [4], and Xiao in 2019 [5] reviewed the biaxial tensile test systems and cruciform samples for sheet metal. Collins et al. in 2015 [6] reported synchrotron X-ray diffraction studies of *in situ* biaxial deformation of steel sheet. Kiriyama et al. in 2019 [7] developed a biaxial tensile testing machine for pulsed neutron experiments. Biaxial tests of biomaterials [8, 9], rubbers polymers [10], composites [11] and rock material [12, 13] had also been widely adopted. Yamanaka et al. [14] recently even applied deep neural network approach to estimate biaxial stress–strain curves of sheet metals.

Biaxial testing systems are mainly divided into two categories: machines with two to four hydraulic actuators [1, 15–17] or screw driven [18] actuators. It should be noted that loading machines with two actuators can only be named as quasi-biaxial, as their service basing on a premise that the installation and the deformation of the samples are

✉ X.Q. Lei
leixianqi@lnm.imech.ac.cn

1 LNM, Institute of Mechanics, Chinese Academy of Sciences, Beijing 100190, China

2 School of Future Technology, University of Chinese Academy of Sciences, Beijing 100049, China

3 School of Engineering Science, University of Chinese Academy of Sciences, Beijing 100049, China

symmetric always. However, this is not usually true. When asymmetric errors occur, a closed-loop control system with two actuators cannot adjust the asymmetric force mathematically. Therefore, a closed-loop control system with at least three actuators under stress control mode is the ideal state for biaxial tests. At present, closed-loop control biaxial machines with four actuators have already been commercially available (Zwich/Roell, Instron and MTS etc.). The other categories are devices that mounted on an existing universal testing machine to transfer the uniaxial load to obtain a simultaneous displacement of the four clamped ends of a cruciform specimen, thus applying a multiaxial loading in its center [19–23]. In addition to the two main categories introduced above, bulge tests [24, 25], round bar under torsion tension/compression [26] and thin-wall tubes subjected to a combination of tension/compression and torsion or internal/external pressure [27] are also applied to generate biaxial stress states. The development of biaxial testing machines, devices and the optimal design of the cruciform samples have been well reviewed by Hannon and Tiernan [3] and many others [4, 5, 28–30].

In this paper, we present an economic yet powerful design of equal-biaxial testing device with a rope-pulley system, which ensures symmetric load and minimizes installation deviation. The latter is a common issue for soft materials undergoing large deformation. When mounted on a commercial universal testing machine with non-contact laser extensometer, the device can realize stress–strain curves of soft materials with excellent repeatability and high fidelity.

Method

Design and Manufacturing of the Biaxial Device

The layout of the designed device is shown in Fig. 1(a). It is composed of a moveable end that imposes loads, and a fixed part where test pieces may be mounted; it also ensures the biaxial constraint during deformation. The moveable end and the fixed part are installed on the loading and fixed end of the universal testing machine with pins. High-density polyethylene (HDPE) line of high strength is selected as the loading rope. The revolve path of the rope through the fixed and movable pulleys is guided by the arrows in Fig. 1(a). Since the force along a rope is equal, we realize equal-stress loading when a displacement control boundary is applied. All components of the device are shown in Fig. 1(b). Cruciform samples (top of Fig. 1(b)) with a dimension of

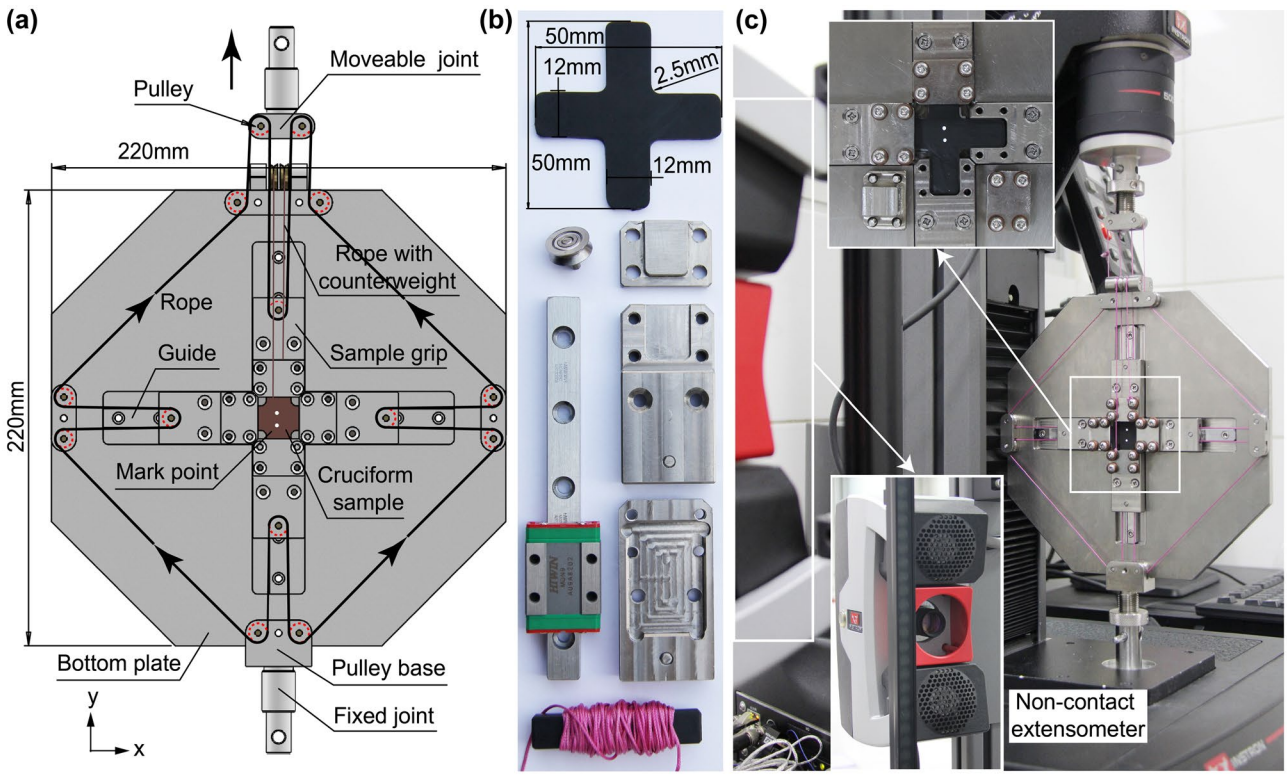

Fig. 1 The layout of an equal-stress biaxial device. (**a**) The device includes both moveable and fixed joints, bottom plate, guides, grips, pulleys, rope. A cruciform sample is placed in the center. (**b**) The dimensions of a cruciform sample and all other components; (**c**) Mounting the biaxial device on a universal testing machine with a non-contact extensometer

50mm × 50mm × 2mm are used, and the central part subject to biaxial loading is 12mm × 12mm. Commercially available V-groove bearings (inner diameter of 3 mm, outer diameter of 12 mm and thickness of 4 mm) and guides are selected as the pulleys and guides of the device. The grips are designed with grooves of 12 mm in width (which matches with the width of cruciform samples). During mounting, disk springs are used to prevent slippage of samples undergoing large deformation. The bottom plate and the grips are made of Ti6Al4V alloy and the weight of the whole device is about 2 kg. The lay out of the device, the mounting process of the cruciform sample, and the location of the Instron AVE non-contacting video extensometer are shown in Fig. 1(c). The strain at the center zone of the cruciform sample is gauged

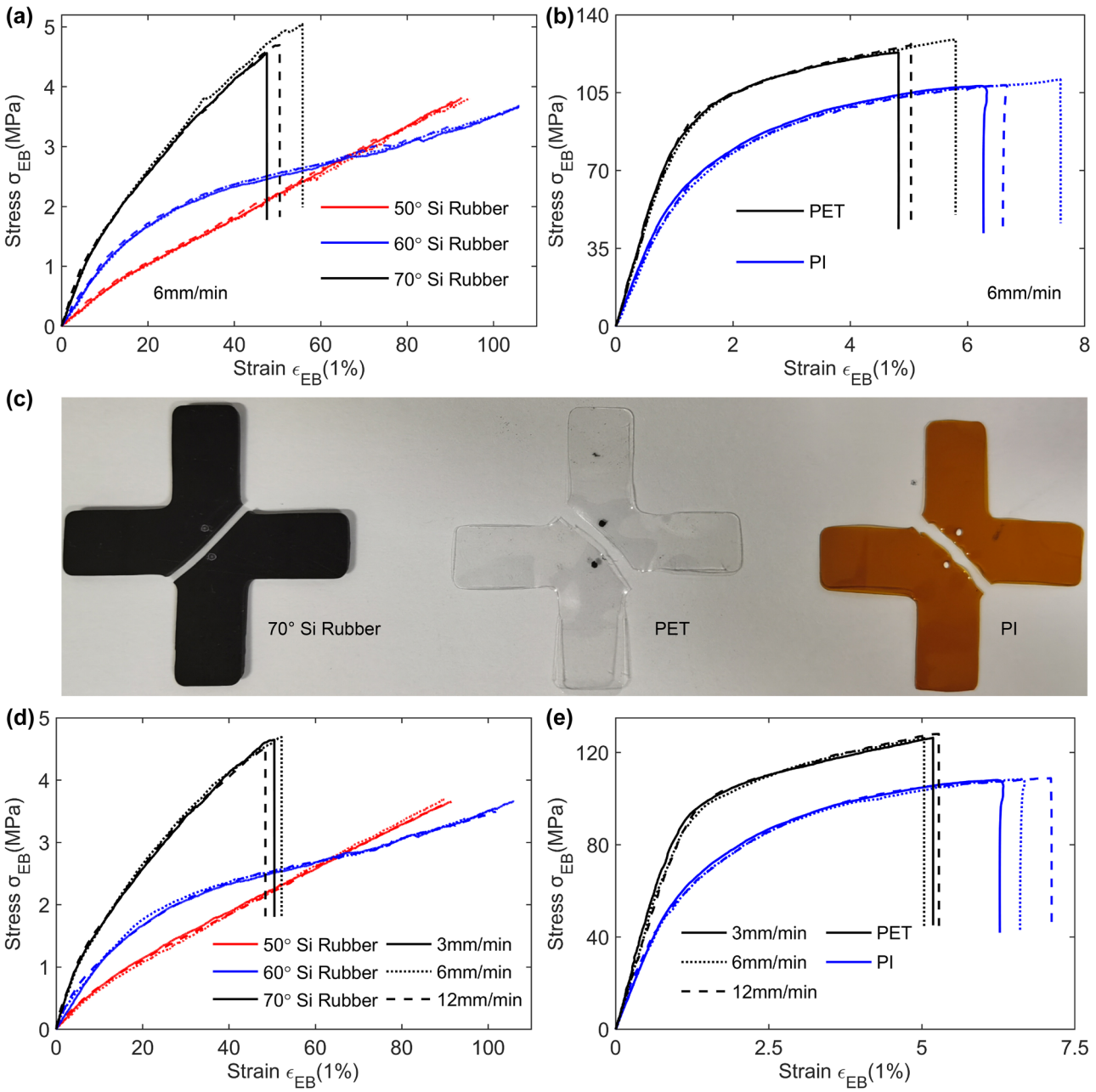

Fig. 2 Stress–strain curves obtained by using the equal-biaxial device. (**a**) Three types of rubbers with different hardness (50°, 60°, 70°). For each type, we carry out three independent tests to examine their repeatability; (**b**) The stress–strain curves of polyimide (PI) and polyethylene terephthalate (PET). In both cases (**a**) and (**b**), the loading speed is 6 mm/min. The subscript EB stands for the equal-biaxial; (**c**) The failure samples with crack across the center region; (**d**) and (**e**) Stress–strain curves under three different loading speeds of 3 mm/min, 6 mm/min and 12 mm/min for three types of rubbers, PI, and PET respectively

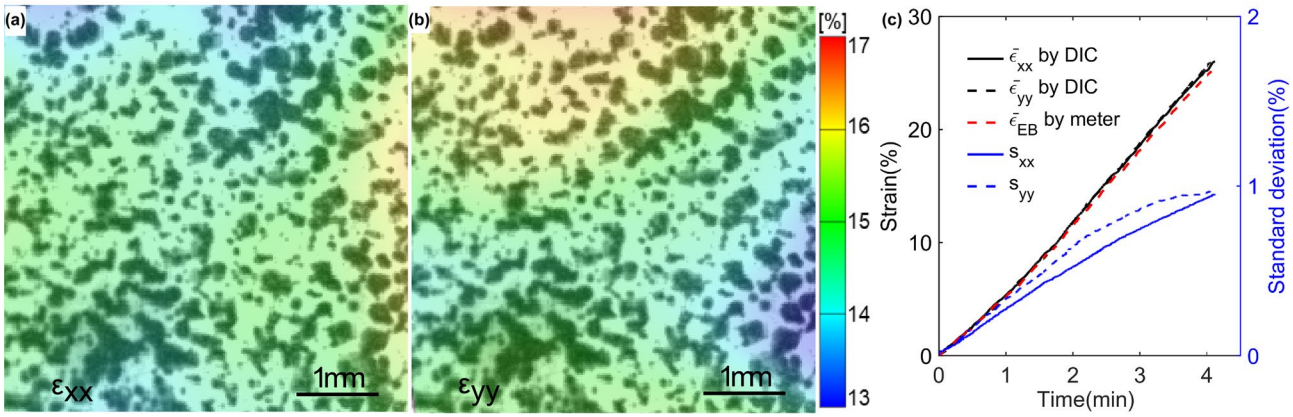

Fig. 3 Equivalence verification between equibiaxial strain and the Y-axis gauged by AVE non-contacting extensometer using digital image correlation (DIC) method. (**a**) and (**b**) strain contours for nominal X-axis strain ε_{xx} and nominal X-axis strain ε_{yy} in the center zone (a 5mm × 5mm square) during our test for 50° rubber; (**c**) The evolution of the average nominal X-axis strain $\bar{\varepsilon}_{xx}$, the average nominal Y-axis strain $\bar{\varepsilon}_{yy}$, and the equibiaxial strain ε_{EB} gauged by the non-contact laser extensometer

by the Instron AVE non-contacting video extensometer. With isotropic elasticity assumption, we use this gauged Y-axis strain to represent the equibiaxial strain of the test materials.

Results and Discussion

Equal-biaxial Test

The equal-biaxial stress–strain curves of rubber materials with three international rubber hardness degrees (IRHD) of 50°, 60° and 70° are shown in Fig. 2(a). For rubber, it is general to use nominal stress and nominal strain [31]: the former represents the nominal equi-biaxial stress in the central region of the cruciform sample, and the latter is obtained from the Instron AVE non-contacting video extensometer. We perform three independent tests for each type of rubber. Except the slight difference in failure strains, each type of rubber exhibits the same stress–strain response. To further verify the applicability of the device, we test two more different soft materials, polyimide (PI) and polyethylene terephthalate (PET).The stress–strain curves are shown in Fig. 2(b) and it can also be seen that the stress–strain curves are repeatable. In Fig. 2(c) the failure samples are shown and the cracks pass through the central region of the cruciform samples. In above cases, the loading speed is keeping at 6 mm/min. We also tried different loading speeds of 3 mm/

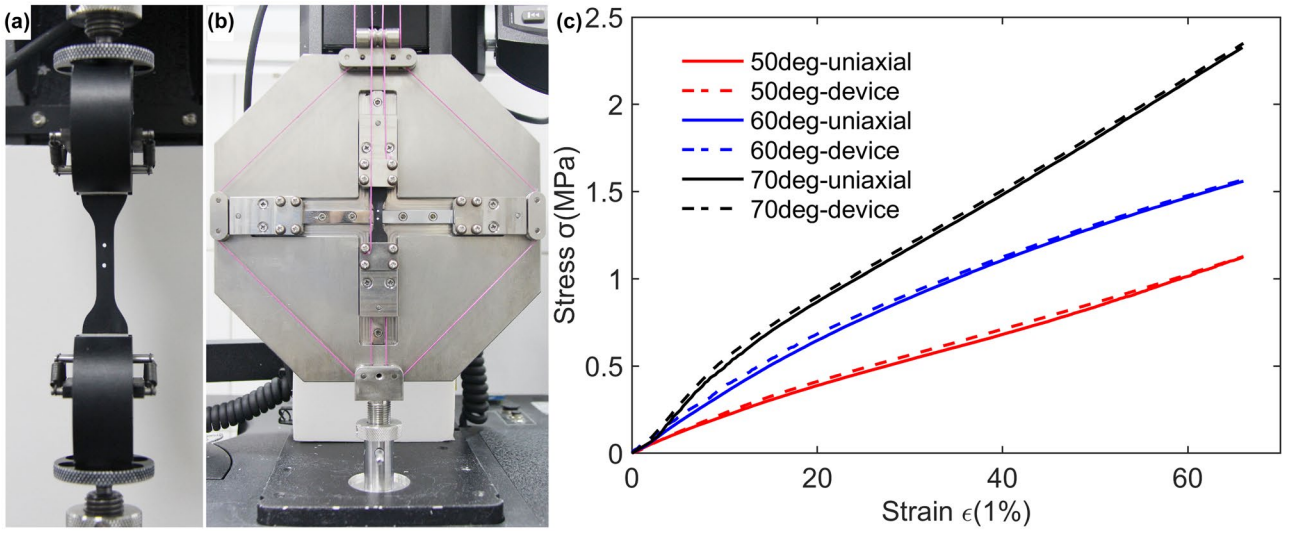

Fig. 4 A comparison of uniaxial tension with commercial testing machine. (**a**) The commercial testing machine (Instron 5942); (**b**) Realizing uniaxial tension using our device by keep the two horizontal slides fixed; (**c**) A comparison of the stress–strain curves of rubbers with three different hardness, the solid line from Instron 5942, and the dashed line from our biaxial device

min and 12 mm/min to verify the reliability of the device. As shown in Fig. 2(d) and (e), the stress–strain curves obtained at 3 mm/min and 12 mm/min match well with that of 6 mm/min, indicating the rate-insensitive nature of the materials.

In order to verify the rationality to use the AVE gauged Y-axis strain to represent the equibiaxial strain of the tests, we further employ digital image correlation (DIC) method to evaluate the equivalence between the Y-axis strain (Fig. 1(a)), X-axis strain (Fig. 1(a)), and the non-contacting extensometer gauged strain (similar verification had also been done by Brieu et al. [22]). The strain at the center region of the cruciform samples is relatively uniform as observed in literature [11, 30, 31]. We choose a 5mm × 5mm center region of the cruciform sample to calculate the strain fields. The nominal X-axis strain ε_{xx} and nominal Y-axis strain ε_{yy} contours are shown in Fig. 3(a) and (b), respectively. The standard deviations of the two strains are lower than 1%. The comparison between the average nominal X-axis strain $\overline{\varepsilon}_{xx}$, average nominal Y-axis strain $\overline{\varepsilon}_{yy}$, and the gauged strain ε_{EB} from the non-contacting extensometer is shown in Fig. 3(c). It can be seen that $\overline{\varepsilon}_{xx}$, $\overline{\varepsilon}_{yy}$ and ε_{EB} agree well with each other during the whole tensile process.

To further evaluate the effectiveness of the device, we compare the stress–strain curves of rubber materials from direct uniaxial tension tests using Instron 5942 (see Fig. 4(a)) with those from the biaxial device. By keeping two horizontal sliders of the designed device fixed and the two vertical sliders free to move, we realize uniaxial tensile

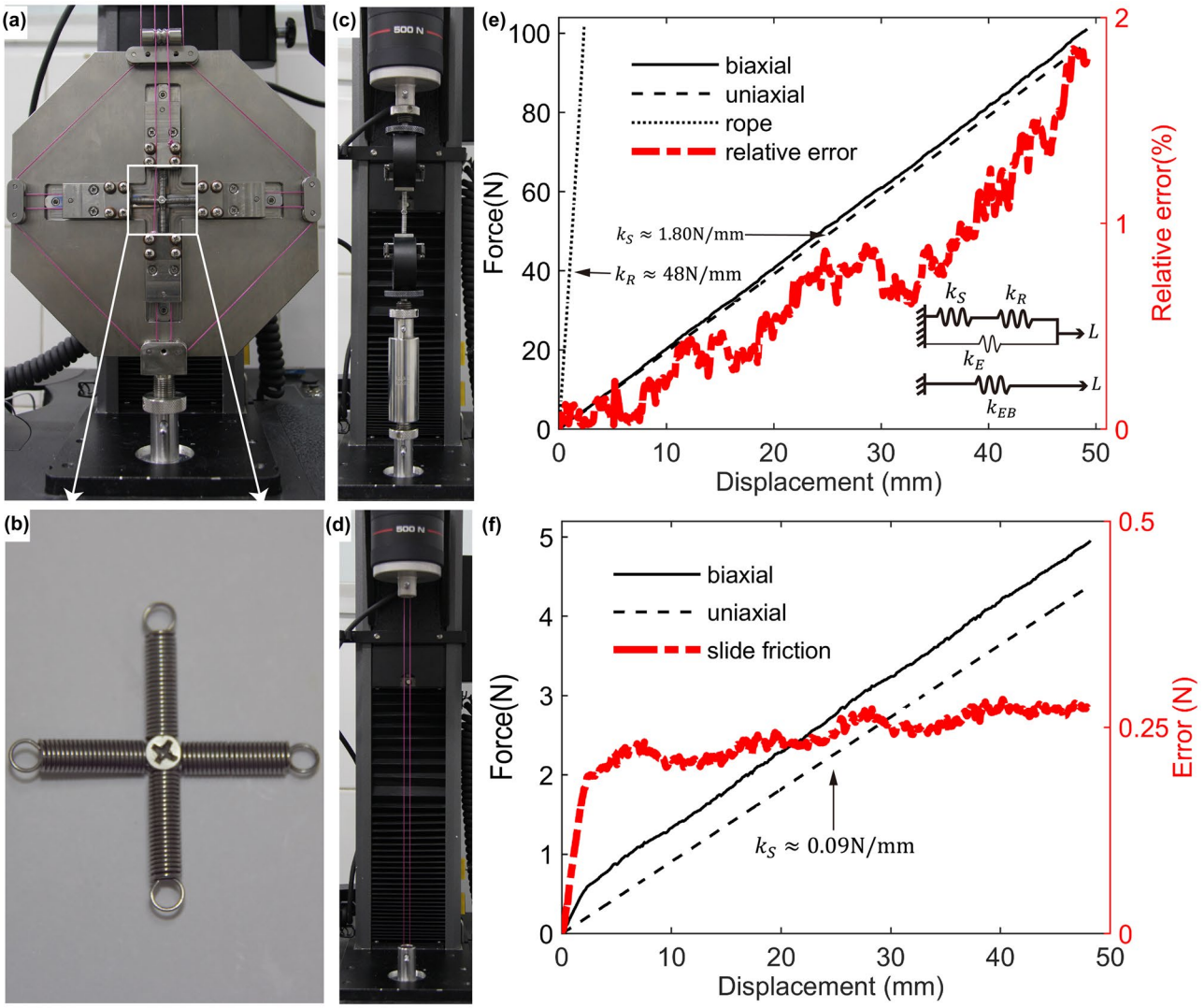

Fig. 5 Error calibration of the equal-biaxial tensile device. (**a**) equibiaxial tension of the four cross springs; (**b**) Close-up view of the four freely pinned springs; (**c**) uniaxial tension of a pair of pinned springs to obtain the its stiffness; (**d**) uniaxial tension of the rope to extract its stiffness k_R and $k_R \approx 48$N/mm; (**e**) the device can be equivalent to a series combination of spring and rope, at same time in parallel with an error, which has a total stiffness k_{EB}. (**f**) The force–displacement curves of the equibiaxial tension (black solid) with spring stiffness of 0.09 N/mm (black dashed). The guide friction (red solid) is found to be 0.25 N within the displacement range of 50 mm

tests in the biaxial device as well, as shown in Fig. 4(b). We show in Fig. 4(c) the stress–strain curves of rubber of different hardness, with solid lines from the direct tensile machine and dashed ones from the biaxial device.

Error Analysis

We design a four-spring tensile method to analyze the errors in the biaxial device. As shown in Fig. 5(a), four springs are used to replace the cruciform samples, and the four springs are cross pinned with a bolt to keep the symmetry of the equibiaxial tension (close-up view in Fig. 5(b)). The device with an equivalent stiffness k_{EB} can be modeled as a series combination of the rope and the calibration spring, at the same time parallel with an error, which include the spring stiffness k_S (Fig. 5(c)), rope stiffness k_R (Fig. 5(d)), and an artificial stiffness k_E accounting for the error of the device. Note the error mainly originates from guide friction and pulley rolling resistance, as seen in Fig. 5(e). By approximation, we may write $k_E = \frac{k_R k_S}{k_S + k_R} - k_{EB}$. We then employ cross springs with stiffness $k_S \approx 1.80\mathrm{N/mm}$ (Fig. 5(e) black dashed, rope stiffness $k_R \approx 48\mathrm{N/mm}$ black dotted) to conduct the equibiaxial tensile calibration tests (Fig. 5(e) black solid); the error stiffness k_E can be obtained from the approximation. Relative error is then derived from the ratio of k_E over k_{EB}, as shown in Fig. 5(e) (red bold dashed). While it keeps increasing with continuing equibiaxial load, the error is lower than 2% at an equibiaxial load of 100 N and a displacement of 50 mm. In order to further understand frictional resistance of the guide to the device, we use low stiffness springs ($k_S \approx 0.09\mathrm{N/mm}$, as shown in Fig. 5(f) black dashed) to conduct the calibration (as Fig. 5(f) black solid). With the stiffness approximation, we obtain an error stiffness k_E on the order of $0.005\mathrm{N/mm}$ (Fig. 5(f) red bold dashed). The friction at each guide is estimated to be 0.25 N at a displacement of 50 mm.

Conclusions

Soft materials with multi-scale structure have been widely utilized in many fields for their compliant nature, including flexible sensors [32] soft robots [33], biological materials [34], biomedical engineering [35, 36], and new material development [37, 38] and so on. Their mechanical response, in particularly under multiaxial stresses, plays a key role and should be known as a prior in engineering practice. Multiaxial testing machines for soft materials are much more expensive than their uniaxial counterparts. This is the reason why multiple options for biaxial loading are available in literature [20–23, 39, 40]. In this work, we design a rope and pulley equipped equal-biaxial device. In combination with a universal testing machine, the device can implement equal-stress constraint and thus overcomes possible deviation from installation and/or due to large deformation. In the rope-pulley device, we apply displacement-controlled loading and overcome those potential deviations often seen in rigid arm devices. We demonstrate, through biaxial tests for rubbers of different hardness, as well as PI and PET, that the device can supply highly repeatable and accurate equal-axial strain–stress curve for such types of soft materials. Given its low cost and high accuracy, it may be applied, with extended loading and displacement range, for many other soft materials including rubbers, polymers, and biomaterials.

Acknowledgements The authors acknowledge support from National Natural Science Foundation of China (NSFC) Basic Science Center for "Multiscale Problems in Nonlinear Mechanics" (Grant 11988102), as well as NSFC Grants 11790291 and 11802308; the Strategic Priority Research Program of the Chinese Academy of Sciences (CAS) (Grant XDB22020200), and CAS Center for Excellence in Complex System Mechanics.

Declarations

Conflicts of Interest The authors declare that they have no conflicts of interest.

References

1. Makinde A, Thibodeau L, Neale KW (1992) Development of an apparatus for biaxial testing using cruciform specimens. Exp Mech 32(2):138–144
2. Kuwabara T (2007) Advances in experiments on metal sheets and tubes in support of constitutive modeling and forming simulations. Int J Plast 23(3):385–419
3. Hannon A, Tiernan P (2008) A review of planar biaxial tensile test systems for sheet metal. J Mater Process Technol 198(1–3):1–13
4. Merklein M, Biasutti M (2013) Development of a biaxial tensile machine for characterization of sheet metals. J Mater Process Technol 213(6):939–946
5. Xiao R (2019) A review of cruciform biaxial tensile testing of sheet metals. Exp Tech 43(5):501–520
6. Collins DM, Mostafavi M, Todd RI, Connolley T, Wilkinson AJ (2015) A synchrotron X-ray diffraction study of *in situ* biaxial deformation. Acta Mater 90:46–58
7. Kiriyama K, Zhang S, Hayashida H, Suzuki JI, Kuwabara T (2019) Development of a biaxial tensile testing machine for pulsed neutron experiments. MethodsX 6:2166–2175
8. Eilaghi A, Flanagan JG, Tertinegg I, Simmons CA, Brodland GW, Ethier CR (2010) Biaxial mechanical testing of human sclera. J Biomech 43(9):1696–1701
9. Sacks MS (2000) Biaxial mechanical evaluation of planar biological materials. J Elast 61(1–3):199–246
10. Sasso M, Palmieri G, Chiappini G, Amodio D (2008) Characterization of hyperelastic rubber-like materials by biaxial and uniaxial stretching tests based on optical methods. Polym Test 27(8):995–1004
11. Smits A, Van Hemelrijck D, Philippidis TP, Cardon A (2006) Design of a cruciform specimen for biaxial testing of fibre reinforced composite laminates. Compos Sci Technol 66(7–8):964–975

12. Arora S, Mishra B (2015) Investigation of the failure mode of shale rocks in biaxial and triaxial compression tests. Int J Rock Mech Min Sci 79:109–123
13. Bobet A, Einstein HH (1998) Fracture coalescence in rock-type materials under uniaxial and biaxial compression. Int J Rock Mech Min Sci 35(7):863–888
14. Yamanaka A, Kamijyo R, Koenuma K, Watanabe I, Kuwabara T (2020) Deep neural network approach to estimate biaxial stress-strain curves of sheet metals. Mater Des 195:108970
15. Crosby (1998) Yield locus of Al–Li sheets under biaxial condition. Paper presented at the Proceedings of the 19th Energy Sources Technology Conference and Exhibition, Houston, USA.
16. Shiratori E, Ikegami K (1967) A new biaxial tensile testing machine with flat specimen. Bull Tokyo Inst Technol 80:105–118
17. Zidane I, Guines D, Leotoing L, Ragneau E (2010) Development of an in-plane biaxial test for forming limit curve (FLC) characterization of metallic sheets. Meas Sci Technol 21(5):055701
18. Boehler JP, Demmerle S, Koss S (1994) A new direct biaxial testing machine for anisotropic materials. Exp Mech 34(1):1–9
19. Ferron G, Makinde A (1998) Design and development of a biaxial strength testing device. J Test Eval 16:253–256
20. Barroso A, Correa E, Freire J, Paris F (2018) A device for biaxial testing in uniaxial machines design manufacturing and experimental results using cruciform specimens of composite materials. Exp Mech 58(1):49–53
21. Bhatnagar N, Bhardwaj R, Selvakumar P, Brieu M (2007) Development of a biaxial tensile test fixture for reinforced thermoplastic composites. Polym Test 26(2):154–161
22. Brieu M, Diani J, Bhatnagar N (2007) New biaxial tension test fixture for uniaxial testing machine - A validation for hyperelastic behavior of rubber-like materials. J Test Eval 35(4):364–372
23. Rohr I, Harwick W, Nahme H (2005) A biaxial cruciform test for the determination of material data of polyamid 6.6 airbag fabric. Materialwiss Werkstech 36(5):195–197
24. Kuwabara T, Sugawara F (2013) Multiaxial tube expansion test method for measurement of sheet metal deformation behavior under biaxial tension for a large strain range. Int J Plast 45:103–118
25. Min J, Stoughton TB, Carsley JE, Carlson BE, Lin J, Gao X (2017) Accurate characterization of biaxial stress-strain response of sheet metal from bulge testing. Int J Plast 94:192–213
26. Lei X, Wei Y, Wei B, Wang WH (2015) Spiral fracture in metallic glasses and its correlation with failure criterion. Acta Mater 99:206–212
27. Lefebvre D, Chebl C, Thibodeau L, Khazzari E (1983) A high-strain biaxial-testing rig for thin-walled tubes under axial load and pressure. Exp Mech 23(4):384–392
28. Demmerle S, Boehler JP (1993) Optimal-design of biaxial tensile cruciform specimens. J Mech Phys Solids 41(1):143–181
29. Pereira AB, Fernandes FAO, Morais AB, Maio J (2020) Biaxial testing machine: development and evaluation. Machines 8(3):40
30. Zhang R, Shao Z, Shi Z, Dean TA, Lin J (2021) Effect of cruciform specimen design on strain paths and fracture location in equi-biaxial tension. J Mater Process Technol 289:116932
31. Fujikawa M, Maeda N, Yamabe J, Kodama Y, Koishi M (2014) Determining stress–strain in rubber with in-plane biaxial tensile tester. Exp Mech 54(9):1639–1649
32. Tee BCK, Ouyang J (2018) Soft electronically functional polymeric composite materials for a flexible and stretchable digital future. Adv Mater 30(47):1802560
33. Jiao Z, Zhang C, Wang W, Pan M, Yang H, Zou J (2019) Advanced artificial muscle for flexible material-based reconfigurable soft robots. Adv Sci 6(21):1901371
34. Yang J, Zhang YS, Yue K, Khademhosseini A (2017) Cell-laden hydrogels for osteochondral and cartilage tissue engineering. Acta Biomater 57:1–25
35. Sharif-Kashani P, Hubschman JP, Sassoon D, Kavehpour HP (2011) Rheology of the vitreous gel: Effects of macromolecule organization on the viscoelastic properties. J Biomech 44(3):419–423
36. Madani N, Mojra A (2017) Quantitative diagnosis of breast tumors by characterization of viscoelastic behavior of healthy breast tissue. J Mech Behav Biomed Mater 68:180–187
37. Kim J, Cote LJ, Huang J (2012) Two dimensional soft material: new faces of graphene oxide. Acc Chem Res 45(8):1356–1364
38. Roy D, Cambre JN, Sumerlin BS (2010) Future perspectives and recent advances in stimuli-responsive materials. Prog Polym Sci 35(1–2):278–301
39. Seymen Y, Guler B, Efe M (2016) Large strain and small-scale biaxial testing of sheet metals. Exp Mech 56(9):1519–1530
40. Guler B, Efe M (2018) Forming and fracture limits of sheet metals deforming without a local neck. J Mater Process Technol 252:477–484